

Proceedings of the 8th Workshop on Quantum Chaos and Localisation Phenomena, May 19–21, 2017, Warsaw, Poland

Experimental Study of Quantum Graphs with Simple Microwave Networks: Non-Universal Features

Z. FU^{a,b}, T. KOCH^c, T.M. ANTONSEN^{a,c}, E. OTT^{a,c} AND S.M. ANLAGE^{a,b,c}

^aDepartment of Electrical and Computer Engineering, University of Maryland, College Park, MD 20742-3285 USA

^bCenter for Nanophysics and Advanced Materials, University of Maryland, College Park, MD 20742-4111 USA

^cDepartment of Physics, University of Maryland, College Park, MD 20742-4111 USA

Quantum graphs provide a setting to test the hypothesis that all ray-chaotic systems show universal wave chaotic properties. Here, an experimental setup consisting of a microwave coaxial cable network is used to simulate quantum graphs. The networks which are large compared to the wavelength, are constructed from coaxial cables connected by T junctions. The distributions of impedance statistics are obtained from experiments on an ensemble of tetrahedral networks. The random coupling model (RCM) is applied in an attempt to uncover the universal statistical properties of the system. Deviations from RCM predictions have been observed in that the statistics of diagonal and off-diagonal impedance elements are different. It is argued that because of the small finite-size quantum graphs utilized here there will be non-universal results.

DOI: [10.12693/APhysPolA.132.1655](https://doi.org/10.12693/APhysPolA.132.1655)

PACS/topics: Quantum graphs, universal fluctuations, impedance, random coupling model, microwave graphs

1. Introduction

A graph or network is a set of elements which are connected in a certain topology. Graphs have applications in many different branches of engineering, science, sociology and biology [1]. A quantum graph, introduced by Pauling in the 1930s, is a linear network structure of vertices connected by bonds with a differential or pseudo-differential operator acting on functions defined on the bonds [2]. In physics, quantum graphs have been used to model many phenomena, such as acoustic and electromagnetic waveguide networks, quantum Hall systems and mesoscopic quantum systems [1]. Researchers have studied quantum graphs experimentally and numerically [3–6]. Quantum graphs have been realized as microwave networks with different topologies such as tetrahedral, irregular hexagon fully connected networks, and fully connected five vertex networks [3–6]. Spectral statistics of graph systems [3, 5], the statistics of the reaction matrix K [4, 5] and the reflection statistics for one-port graphs [4, 5], and the impedance statistics of networks of complex enclosures [7], have been studied and results from both numerical calculation and experimental measurement show good agreement with theory.

In this paper, investigations and study are mainly focused on the impedance statistics of a two-port tetrahedral microwave graph. The microwave networks, with bonds that are large compared with the wavelength, are constructed from coaxial cables connected by T junctions [3–6]. The graph is open with two coupled ports. Scattering matrices which describe the electromagnetic wave scattering properties of the networks are measured by a microwave vector network analyzer.

The random coupling model (RCM) [8] has been introduced to describe the impedance statistics of single- and multi-port wave chaotic systems. In this work we compare the predictions of the RCM with our measure-

ments of an ensemble of tetrahedral graphs. The RCM posits that the measured impedance of the complex wave-chaotic system is made up of a universally-fluctuating part, dressed by a system-specific radiation impedance matrix. The radiation impedance captures the radiating properties of the ports (through the real part), and the energy stored in the near-field of the ports (through the imaginary part). Losses in the system are assumed to be homogeneous, giving rise to a single finite quality factor for all the modes of the closed system. The key parameter in the RCM is the loss parameter α , which determines the probability density of the universally-fluctuating complex impedance [9, 10].

In our experiments, an ensemble of graphs is created and the complex impedance of each realization is measured as a function of excitation frequency through the two ports. Next, the average of the measured impedance over all these realizations is compiled. This averaged impedance quantity captures both the radiation impedance of the ports and the contributions of short orbits between the ports [11, 12]. We then take the measured impedance and normalize it (i.e. remove the effects of the port radiation impedances and short orbits) to examine a fluctuating impedance. In the case of wave chaotic systems it is expected that the normalized impedance has a probability density function (PDF) that is described by Random Matrix Theory (RMT), and this PDF is governed by a single parameter, namely the loss parameter α [11–14]. In principle, one can then fit the normalized impedance (real and imaginary) data PDFs to RMT and determine α as a fitting parameter. To independently determine the loss parameter α , two techniques are employed. The first is to take the measured scattering parameter data as a function of frequency and Fourier transform it into the time domain [15]. One can estimate the quality factor of the graph from the decay

of energy in the graph, and from this the loss parameter can be estimated. In addition, the microwave networks are simulated numerically to estimate the loss parameter α of the network.

In the remainder of the paper we first review the key properties of the Random Coupling Model as applied to understanding the statistical properties of wave chaotic systems through the electrical impedance. Next we discuss the experimental realization of an ensemble of tetrahedral graphs and the measurements performed. We also introduce a numerical simulation that closely mimics the properties of the experimental system. Next we go through representative experimental results and discuss the degree to which the fluctuations in normalized impedance show universal behavior. Finally we discuss the results and conclude

2. Random Coupling Model (RCM)

The random coupling model (RCM) describes the coupling of radiation into and out of electrically large enclosures with chaotic ray dynamics [8]. The RCM gives a prescription for determining both the universal and non-universal features of the experiment. The RCM has successfully analyzed the statistical properties of the impedance (\hat{Z}) and scattering (\hat{S}) matrices of open electromagnetic cavities where the waves are coupled through transmission lines or waveguide [13]. In [11, 14], a 2D ray-chaotic quarter-bowtie cavity and in [16] a 3D complex ‘‘GigaBox’’ cavity have been studied and impedance statistics have been analyzed from experimental measurement. In this paper, the RCM is applied for the analysis of electromagnetic propagation in quasi-1D microwave networks.

In the RCM, the statistics of the impedance matrix, \hat{Z}_{cav} of a ray-chaotic cavity in the semi-classical limit can be obtained from the universal and system-specific properties of the cavity as [8,–10, 14]

$$\hat{Z}_{cav} = i\text{Im}[\langle \hat{Z}_{cav} \rangle] + \text{Re}[\langle \hat{Z}_{cav} \rangle]^{1/2} \hat{z} \text{Re}[\langle \hat{Z}_{cav} \rangle]^{1/2}. \quad (1)$$

The matrix $\langle \hat{Z}_{cav} \rangle$ is the ensemble-averaged cavity impedance matrix, which describes the system-specific features, including the radiation impedance of the ports and short-orbits that exist in the ensemble [12]. Short orbits are trajectories that go from a port and bounce a few times before the energy leaves the graph through the same port or another port. This should be contrasted with longer orbits, which contribute to the universal impedance fluctuations.

The matrix \hat{z} in Eq.(1) is the normalized impedance, the statistical properties of which can be predicted by random matrix theory, and the \hat{z} matrix describes the universal fluctuation properties of the system.

In [8], the normalized impedance \hat{z} can be modelled as,

$$\hat{z}(k_0) = -\frac{i}{\pi} \sum_n \frac{\phi_n \phi_n^T}{\frac{k_0^2 - k_n^2}{\Delta k^2} + i\alpha}, \quad (2)$$

where ϕ_n is a vector of length M for an M -port sys-

tem. The elements of ϕ_n are the variables describing the coupling of each mode n to the ports. If we assume that the Berry hypothesis [17] applies then on average the statistical properties of the fields at any point inside the system are described by a random superposition of plane waves of all possible directions and phases. Based on this hypothesis we take the ϕ_n to be Gaussian random variables, which follows from the random plane-wave hypothesis, and this assumption will be called into question for finite-size graphs later in the paper. Also, Δk^2 is the mean mode spacing of the closed system, k_n are the cavity mode wavenumbers and k_0 is the wavenumber of interest. We take the spectrum of eigenmodes k_n to be that of a Gaussian orthogonal random matrix. The statistical fluctuating properties of the normalized impedance \hat{z} in the RCM is determined by a single loss parameter α defined as

$$\alpha = \frac{k_0^2}{\Delta k^2 Q}, \quad (3)$$

where Q is the quality factor of the closed cavity or network. The losses are assumed uniformly distributed in the graph, and the variation of the Q from one mode to the next is expected to be small, so that an average Q meaningfully quantifies the degree of loss. The loss parameter can also be thought of as the ratio of the 3-dB bandwidth of a typical mode to the mean spacing of the modes. As such, the loss parameter is a slowly varying function of frequency in most systems. A lossless system has $\alpha = 0$, and typical over-moded reverberant systems encountered in real life have loss parameters between 0.1 and 10.

The loss parameter α can be calculated directly through knowledge of the average quality factor and mode-spacing over a certain frequency range. This gives an alternate way which can be compared with the loss parameter obtained from fitting PDFs of normalized impedance \hat{z} extracted from experimental data.

3. Experimental setup and data analysis

The experimental setup is shown in Fig.1. Coaxial cables are connected by the T junctions to form a tetrahedral network. For the coupling ports, two T junctions are connected to form the 4-coaxial-connector junction. Each cable used in the graph has a unique length. The minimum length of the cables is 1.0 m and maximum is 1.5 m with the average length of 1.3 m. Hence the total length of the networks is around 7.8 m. And for the frequency range we have measured, the wavelengths range from 0.01 m to 0.05 m, making the graph electrically large and highly over-moded. A network analyzer is connected to two ports of the network and the 2 by 2 scattering matrix is measured as a function of frequency (or wavenumber) from 1 GHz to 18 GHz where there is a single mode of propagation in the network.

To achieve a randomized electromagnetic environment and a high quality ensemble of the microwave networks, different realizations are generated in the experiment.

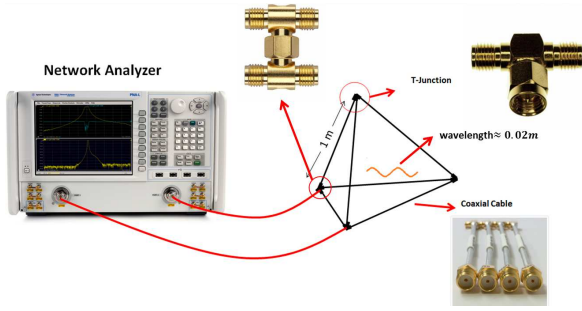


Fig. 1. Experimental setup of the microwave networks. The network analyzer (left) is connected to the tetrahedral graph by means of two coaxial cables (shown in red). The ports are made up of two tee-junctions (inset), while the other nodes are simple tee-junctions (upper right inset).

The system is perturbed globally by changing the total length of the network. In each member of the ensemble one of the bonds is changed to another cable of a different unique length and in all about 80 unique realizations are created. To test the quality of this ensemble, the ratio A of the maximum transmitted power to the minimum transmitted power at each frequency point for the different realizations is compiled [14].

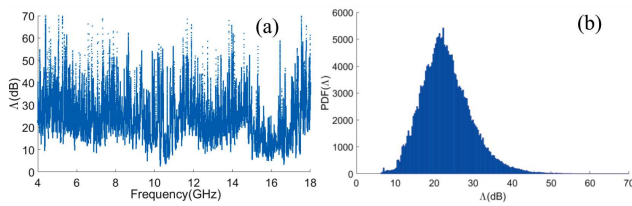


Fig. 2. (a) Plot of A vs. frequency for an ensemble of 81 realizations of the tetrahedral microwave graph. A value of A is found for every measured frequency point between 4 and 18 GHz. (b) Histogram of the ratio A of the maximum transmitted power to the minimum transmitted power over an ensemble of 81 realizations of the tetrahedral graph.

In Fig. 2 we can see that the histogram of A is widely spread with a mean of 23 dB and a standard deviation of 6.5 dB. The dynamic range of A over the frequency range of 4 to 18 GHz is about 60 dB, and this shows that the ensemble is of high quality and suitable for further statistical analysis [18].

A numerical simulation model of the tetrahedral network is also set up in the Computer Simulation Technology (CST) software. Following the same procedure as in the experimental measurements, the 2 by 2 scattering matrix as a function of frequency can be obtained from the numerical calculation. In this model, the two main modules are the coaxial cable and T-junction. For the coaxial cable block, the parameters for the resistance, dielectric constant, inner and outer diameter of the coaxial cable model are all adjusted to make the S-parameters of

the block as close as possible to those of the cables used in the experiment. The lengths of the coaxial cables can be easily changed during the simulation which allows us to efficiently generate an ensemble of the networks. A Touchstone file with directly measured S-parameter data as a function of frequency is imported as the block for the T-junction. Thus the numerical simulation provides a close approximation to the experiment.

4 Experimental results

The raw data can be examined to yield insights for use in the RCM analysis. Fig. 3 shows the resistance and reactance of three kinds of impedance obtained from the measured raw data in the 9 to 10 GHz subset of the data. The blue (strongly fluctuating) curve is the impedance of one realization of the network, labeled as Z . The red (gently fluctuating) curve is the impedance averaged over all the realizations of the graph, labeled as Z_{avg} . The green (smooth) curve is the measured radiation impedance of the ports, labeled as Z_{rad} . The radiation impedance Z_{rad} was measured by removing the graph in Fig. 1 and placing absorptive loads on the three open coaxial connectors of the two ports. From the plots, we can see that Z and Z_{avg} are both fluctuating around the slowly-varying Z_{rad} . The small oscillations in Z_{avg} are manifestations of the short-orbits that survive in many realizations of the networks [19].

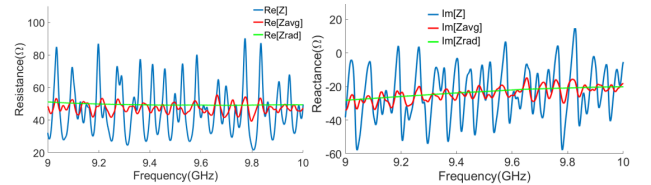


Fig. 3. Resistance and reactance (real and imaginary parts of impedance) of one realization of a tetrahedral graph network (blue, large amplitude fluctuations, labeled Z), averaged impedance over all realizations (red, intermediate amplitude fluctuations, labeled Z_{avg}) and measured radiation impedance (green, smooth curve, labeled Z_{rad}) from 9 to 10 GHz.

As described in section 2, the measured scattering matrix ensemble data can be used to examine the statistics of the normalized impedance matrix \hat{z} in Eq. (1) and compared to the predictions of RMT in Eq. (2). The matrix $\langle \hat{Z}_{cav} \rangle$ is computed by taking the average of the measured Z_{cav} over all the realizations at each frequency point. The impedance matrix \hat{z} is obtained by solving Eq. (1) using the measured matrix \hat{Z}_{cav} along with $\langle \hat{Z}_{cav} \rangle$. As shown in Fig. 3, the averaged impedance $\langle \hat{Z}_{cav} \rangle$ includes the radiation impedance along with the short-orbits effects in the network. The normalization process is expected to remove the non-universal coupling of the ports and the short-orbit effects in the networks, and based on the RCM the normalized impedance matrix \hat{z} is expected to display universal statistical properties.

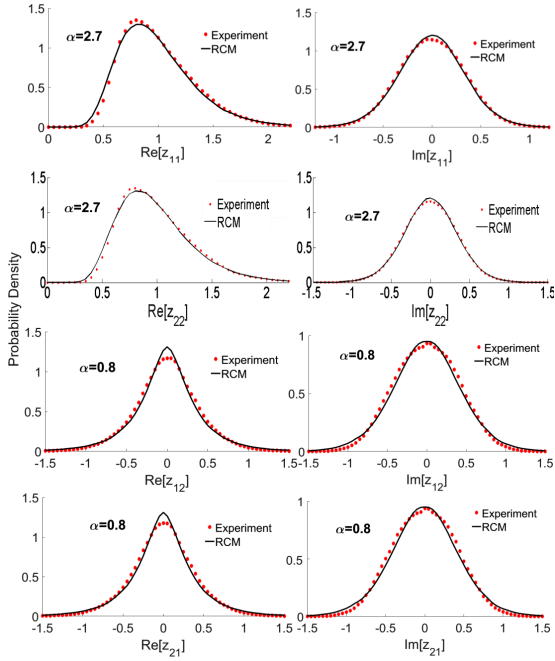


Fig. 4. PDFs of the real and imaginary parts of z_{11} , z_{22} , z_{12} and z_{21} from experimental measurements of tetrahedral graphs (red dots) and best fit RCM predictions (black solid lines) with associated α values. The data are from measurements over a frequency range from 4 to 12 GHz.

We can examine the statistics of diagonal and off-diagonal impedance \hat{z} elements, as shown in Fig. 4 over a large frequency range of 4 to 12 GHz. Over this range the loss parameter of the graphs is expected to vary in a smooth and monotonic manner. In the Appendix, an investigation by means of RCM numerical calculations shows that it is reasonable that the RCM can describe the impedance statistics of data resulting from a composite of different loss parameters.

First we note that all of the PDFs in Fig. 4 can be fit to the PDFs predicted by RMT as long as the loss parameter is allowed to vary. In particular, note that the same loss parameter can be used to fit both the real and imaginary data for a given impedance matrix element (namely z_{11} , z_{22} , z_{12} and z_{21}). It is expected that all impedance matrix elements should have statistics governed by a single value of the loss parameter. However, we note that different loss parameters are required to fit the impedance statistics of diagonal (z_{11} , z_{22}) and off-diagonal (z_{12} , z_{21}) elements. In Fig. 4, the PDFs of z_{11} and z_{22} are best fit to RMT with a loss parameter $\alpha = 2.7$, while the PDFs of z_{12} and z_{21} are best fit to RMT with $\alpha = 0.8$. Note that the loss parameters fitting the two diagonal elements (z_{11} and z_{22}), and the two off-diagonal elements (z_{12} and z_{21}) are the same for both real and imaginary parts.

In [16], the RCM was successfully applied to describe the electromagnetic statistics in complex three-dimensional enclosures. However, non-universal behavior

similar to that observed here has also been seen in a 3D cavity case [20], where the enclosures have one wall with an electrically-large aperture. In that case any ray inside the cavity that reaches the aperture will exit the system, leading to a source of loss that is not homogeneous. This also leads to the situation that the Berry random plane-wave hypothesis may not be obeyed for waves at the ports.

To get deeper insight into the data, the numerical simulation results in CST are treated the same way as the data, and the resulting statistical properties of the impedance matrix elements are presented in Fig. 5.

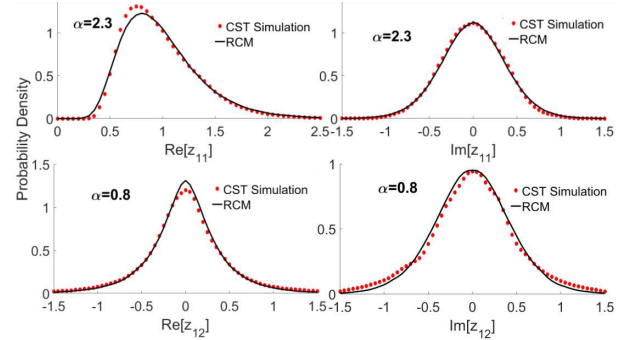


Fig. 5. PDFs of the real and imaginary parts of z_{11} and z_{12} from numerical simulation of tetrahedral graphs (red dots) and RCM fit predictions (black solid lines) along with best-fit α values. The data are from calculations in the frequency range from 6 to 8 GHz.

Numerical calculation results show a number of similar features to the data. First there is good agreement with RMT predictions for the PDFs. In addition, the same value for the loss parameter fits both the real and imaginary statistical fluctuations for a given impedance matrix element. However, the same difference in loss parameter fit value between diagonal and off-diagonal impedance matrix elements is seen as in the experimental measurements. In both cases the PDFs of diagonal impedance elements show a higher loss parameter fit value than the off-diagonal impedance elements. It should be noted that a similar difference in loss parameter values was observed in 3D enclosures with electrically-large apertures [20].

An independent method to directly calculate the loss parameter of the networks is to determine the quality factor Q and, based on Eq. 3 evaluate the loss parameter based on the known wavenumber and mean mode spacing of the graph. A time domain method is applied to determine the quality factor Q for a given frequency range, as illustrated in Fig. 6.

In Fig. 6, the inverse Fourier transforms of both measured S_{11} and S_{12} averaged over all realizations are plotted in the time domain. The averaged quality factor computed from both spectra is $Q = 394$ for the frequency range from 4 to 12 GHz using the equation $Q = \omega\tau$, where ω is the median value of the frequency range. In Eq. 3, k is chosen as the median value for the frequency

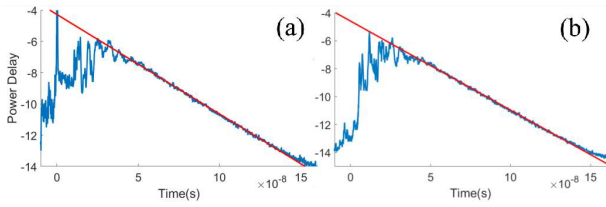


Fig. 6. Inverse Fourier transform of the measured (a) S_{11} and (b) S_{12} averaged over all realizations to compute the decay time τ for the frequency range 4 to 12 GHz. Both data sets give a clear and consistent single decay time of 7.8 ns, determined from a straight line fit shown in red.

range, and the loss parameter obtained by this method is $\alpha_Q = 1.1$, which is close to the value fitting the PDFs of the real and imaginary of the off-diagonal impedance matrix elements z_{12} and z_{21} in Fig. 4.

5. Discussion

Plúhar and Weidenmüller [21] recently showed conditions for universal behavior in quantum graphs and the statistical equivalence to RMT. In [22, 23], experiments with microwave networks are carried out and showed non-universal behavior for long-range fluctuating properties. According to theory, the universal behavior is obtained only in the limit of infinitely intricate graphs with infinitely many bonds and nodes [21]. Field-theoretical results for spectral statistics in finite quantum graphs have largely focused on the size of these deviations, and criteria for their disappearance in the limit of large graphs [21, 24]. Numerical work shows that many statistical properties of finite-size graphs are consistent with random matrix theory, but others, such as the second-order level velocity autocorrelation functions and the parametric curvature distribution, are not in agreement [25]. In this study, the simple and small tetrahedral networks in the experiment have a finite number of elements, and deviations from universal behavior are therefore not unexpected. In fact, some particularly simple graphs, like the star graph, can show entirely non-universal behavior [26]. In this experimental study, the impedance statistics of tetrahedral graphs show some results similar to the universal behavior but also some clear deviations from RMT.

6. Conclusions

In this paper an experimental study of very simple and small quantum graphs simulated by microwave networks is carried out. The statistical properties of the impedance matrix of a 2-port tetrahedral graph ensemble display many properties qualitatively consistent with random matrix theory. However, a non-universal feature is observed for the impedance statistics. Numerical simulations of similar graphs show very similar non-universal statistical properties. It is argued that because of the small finite-size quantum graphs utilized here there will be non-universal results.

7. Appendix, Random Coupling Model impedance statistics with different loss parameter values

In this paper, the experimental data used for the plots of normalized impedance are from a large frequency range of 4 to 12 GHz, over which the loss parameter governing the statistical fluctuations of the impedance is known to vary. In this appendix, we investigate the validity of an RCM treatment of data over a broad frequency range with varying α and show that it is reasonable to analyze this data with a single effective loss parameter value.

The normalized impedance statistics used below are numerically calculated based on the RCM for different α values.

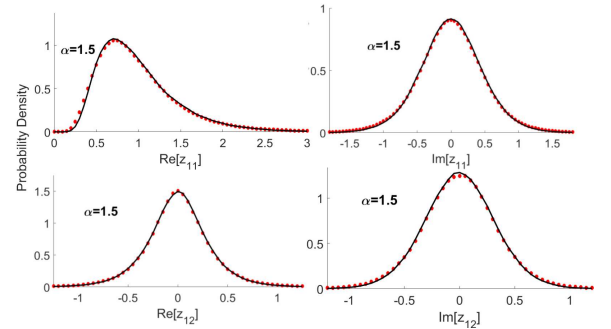


Fig. 7. PDFs of the real and imaginary parts of z_{11} and z_{12} from a composite of normalized impedance statistics of $\alpha = 1$, $\alpha = 2$ (red dots) and normalized RMT impedance statistics (black solid lines) of a single α value. The value of α was determined by fits of the composite PDFs to RMT using α as the fitting parameter.

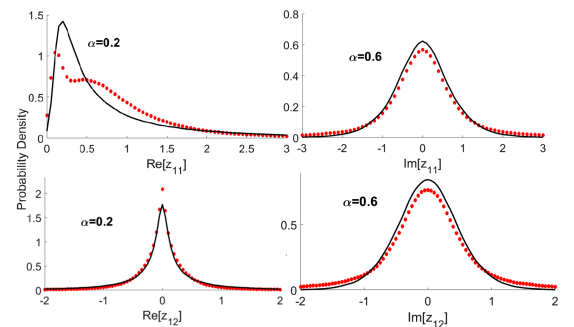


Fig. 8. PDFs of the real and imaginary parts of z_{11} and z_{12} from a composite of normalized impedance statistics of $\alpha = 0.1$, $\alpha = 1$ (red dots) and normalized RMT impedance statistics (black solid lines) of several best-fit α values.

In Fig. 7, the red dots are a composite data set consisting of equal contributions from two data sets with $\alpha = 1$ and $\alpha = 2$. This composite data set was normalized and fit to RMT using α as a fitting parameter. From the plots, we can see that the PDFs of the real and imaginary parts of z_{11} and z_{12} are simultaneously fit (black solid lines) by RMT with a single loss parameter, $\alpha = 1.5$.

However, in Fig. 8 when we create another composite data set from two data sets with $\alpha = 0.1$ and $\alpha = 1$ the PDFs deviate far from the RMT predictions and no single governing loss parameter can be determined. In general we find that composite data sets can be fit well when the PDFs making up those data have similar variances. Since the variance scales roughly inversely with the loss parameter [14], those data sets with $\alpha > 1$ generally are fit well to a single α value for the composite.

Acknowledgments

This work is supported by ONR under Grant No. N000141512134, AFOSR under COE Grant FA9550-15-1-0171, and the Maryland Center for Nanophysics and Advanced Materials.

References

- [1] S. Gnutzmann, U. Smilansky, *Adv. Phys.* **55**, 527 (2006).
- [2] M. Freedman, L. Lovász, A. Schrijver, *J. Amer. Math. Soc.* **20**, 37 (2007).
- [3] O. Hul, S. Bauch, P. Pakoński, N. Savytsky, K. Życzkowski, L. Sirko, *Phys. Rev. E* **69**, 056205 (2004).
- [4] M. Lawniczak, O. Hul, S. Bauch, P. Seba, L. Sirko, *Phys. Rev. E* **77**, 056210 (2008).
- [5] M. Lawniczak, S. Bauch, O. Hul, L. Sirko, *Phys. Scr. T* **135**, 014050 (2009).
- [6] M. Lawniczak, S. Bauch, O. Hul, L. Sirko, [dorefl0.1088/0031-8949/2011/T143/014014](https://doi.org/10.1088/0031-8949/2011/T143/014014) *Phys. Scr. T* **143**, 014014 (2011).
- [7] X. Li, C. Meng, Y. Liu, E. Schamiloglu, S.D. Hemmady, *IEEE Trans. Electromag. Compat.* **57**, 448 (2015).
- [8] G. Gradoni, J.-H. Yeh, B. Xiao, T.M. Antonsen, S.M. Anlage, E. Ott, *Wave Motion* **51**, 606 (2014).
- [9] X. Zheng, T.M. Antonsen Jr., E. Ott, *Electromagnetics* **26**, 3 (2006).
- [10] X. Zheng, T.M. Antonsen Jr., E. Ott, *Electromagnetics* **26**, 37 (2006).
- [11] J.-H. Yeh, J. Hart, E. Bradshaw, T. M. Antonsen, E. Ott, S.M. Anlage, *Phys. Rev. E* **81**, 025201 (2010).
- [12] J.A. Hart, T.M. Antonsen, E. Ott, *Phys. Rev. E* **80**, 041109 (2009).
- [13] X. Zheng, S. Hemmady, T.M. Antonsen Jr., S.M. Anlage, E. Ott, *Phys. Rev. E* **73**, 046208 (2006).
- [14] S. Hemmady, X. Zheng, E. Ott, T.M. Antonsen, S.M. Anlage, *Phys. Rev. Lett.* **94**, 014102 (2005).
- [15] B.D. Addissie, J.C. Rodgers, T.M. Antonsen Jr., 2015 IEEE Metrology for Aerospace (MetroAeroSpace), pp.214-219, DOI: [IEEE Metrology for Aerospace \(MetroAeroSpace\)](https://doi.org/10.1109/MetroAeroSpace.2015.7392144), Benevento 2015, p. 214.
- [16] Z.B. Drikas, J. Gil Gil, S.K. Hong, T.D. Andreadis, J.-H. Yeh, B.T. Taddese, S.M. Anlage, *IEEE Trans. Electromag. Compat.* **56**, 1480 (2014).
- [17] M.V. Berry, *Les Houches Summer School 1981 on Chaotic Behaviour of Deterministic Systems*, Eds.: G. Iooss, H.G. Helleman, R. Stora, North-Holland, Amsterdam 1983, p. 171.
- [18] S. Hemmady, T.M. Antonsen Jr., E. Ott, S.M. Anlage, *IEEE Trans. Electromag. Compat.* **54**, 758 (2012).
- [19] J.-H. Yeh, J.A. Hart, E. Bradshaw, T.M. Antonsen, E. Ott, S.M. Anlage, *Phys. Rev. E* **82**, 041114 (2010).
- [20] J. Gil Gil, Z.B. Drikas, T.D. Andreadis, S.M. Anlage, *IEEE Trans. Electromag. Compat.* **58**, 1535 (2012).
- [21] Plühar, H. Weidenmuller, *Phys. Rev. Lett.* **110**, 034101 (2013).
- [22] B. Dietz, V. Yunko, M. Bialous, S. Bauch, M. Lawniczak, L. Sirko, *Phys. Rev. E* **95**, 052202 (2017).
- [23] M. Bialous, V. Yunko, S. Bauch, M. Lawniczak, B. Dietz, L. Sirko, *Phys. Rev. Lett.* **117**, 144101 (2016).
- [24] S. Gnutzmann, A. Altland, *Phys. Rev. E* **72**, 056215 (2005).
- [25] O. Hul, P. Seba, L. Sirko, *Phys. Rev. E* **79**, 066204 (2009).
- [26] T. Kottos, U. Smilansky, *J. Phys. A: Math. Gen.* **36**, 12 (2003).